

See discussions, stats, and author profiles for this publication at: <https://www.researchgate.net/publication/250082966>

CAHVOR camera model and its photogrammetric conversion for planetary applications

Article *in* Journal of Geophysical Research Atmospheres · April 2004

Impact Factor: 3.43 · DOI: 10.1029/2003JE002199

CITATIONS

25

READS

68

2 authors, including:



[Kaichang Di](#)

Chinese Academy of Sciences

130 PUBLICATIONS 1,242 CITATIONS

SEE PROFILE



CAHVOR camera model and its photogrammetric conversion for planetary applications

Kaichang Di and Rongxing Li

Mapping and GIS Laboratory, Civil and Environmental Engineering and Geodetic Science, Ohio State University, Columbus, Ohio, USA

Received 10 October 2003; revised 17 March 2004; accepted 13 March 2004; published 22 April 2004.

[1] CAHVOR is a camera model used in machine vision for three-dimensional measurements. It models the transformation from the object domain to the image domain using vectors \mathbf{C} , \mathbf{A} , \mathbf{H} , and \mathbf{V} and corrects radial lens distortions with a vector \mathbf{O} and a triplet \mathbf{R} . In photogrammetric mapping the camera model is usually represented by collinearity equations with interior and exterior orientation parameters. In NASA's planetary missions the CAHVOR model has been widely used for rover navigation and scientific exploration. On the other hand, a photogrammetric model is often needed in mapping and photogrammetric data processing systems. This paper presents a method for conversions between the CAHVOR model and the photogrammetry model. A numerical example is given to validate the conversion equations. **INDEX TERMS:** 1224 Geodesy and Gravity; Photogrammetry; 0933 Exploration Geophysics; Remote sensing; 0910 Exploration Geophysics: Data processing; **KEYWORDS:** CAHVOR, camera model, photogrammetry

Citation: Di, K., and R. Li (2004), CAHVOR camera model and its photogrammetric conversion for planetary applications, *J. Geophys. Res.*, 109, E04004, doi:10.1029/2003JE002199.

1. Introduction

[2] In photogrammetric mapping and machine vision, a transformation between the image domain and the three-dimensional (3-D) object domain is a critical step in reconstruction of 3-D objects from stereo images. This transformation is generally realized by a camera (sensor) model, which reconstructs the geometric setting at the time of imaging. In photogrammetry, the camera model is usually represented by collinearity equations with interior orientation (IO) and exterior orientation (EO) parameters [Wolf, 1983; Mikhail *et al.*, 2001]. For high-precision applications, lens distortion parameters are also included to correct the measured image coordinates. Three rotation angles and three translations are explicitly defined as EO parameters. A variation of the collinearity model is the so-called DLT (Direct Linear Transform) that is especially widely used in close-range photogrammetry. The DLT model and the collinearity model can be converted from one to the other [Karara, 1989; Mikhail *et al.*, 2001].

[3] CAHVOR and its subset CAHV are camera models used in machine vision. They have also been extensively used in planetary exploration missions, such as the 1997 Mars Pathfinder (MPF) Mission and the 2003 Mars Exploration Rover (MER) mission. Initiated by Yakimovsky and Cunningham [1978], the CAHV model represents the transformation from object coordinates to image coordinates with four vectors: \mathbf{C} , \mathbf{A} , \mathbf{H} and \mathbf{V} . Later, Gennery [1992] extended the model to the CAHVOR model by including radial lens distortions with a vector \mathbf{O} and a triplet \mathbf{R} . He

also provided a least squares adjustment algorithm for camera calibration.

[4] Although the CAHVOR model and the photogrammetric model have different parameters, they represent the same imaging geometry and may be converted from one model to another at a useful working level of precision. This conversion is needed in many practical situations where the calibration is performed using one camera model while the 3-D reconstruction uses the other. Vast amounts of orbital, lander and rover images acquired by NASA's planetary missions are archived in the Planetary Data System (PDS) and distributed for scientific research and education purposes. Most of the lander and rover camera calibration results stored in PDS are in the CAHVOR format. Photogrammetric processing of such data is very important for supporting geodetic frameworks, precision orbital image processing, and landed planetary applications. Much of the mapping and photogrammetric processing software is developed on the basis of the photogrammetric models. Therefore conversions between the CAHVOR model and the photogrammetric model become an inevitable process in such a multicamera model-based computation. For example, to process the lander and rover images for landing site mapping and rover localization [Kirk *et al.*, 1999; Li *et al.*, 2002, 2004], IO, EO and lens distortion parameters of images were calculated from the corresponding CAHVOR model, which can then be used in a photogrammetric bundle adjustment.

[5] This paper investigates the relationship between the CAHVOR model and the photogrammetric model. An analysis of corresponding parameters of the two models and a conversion between the models are presented. A numerical example is given to show the computations

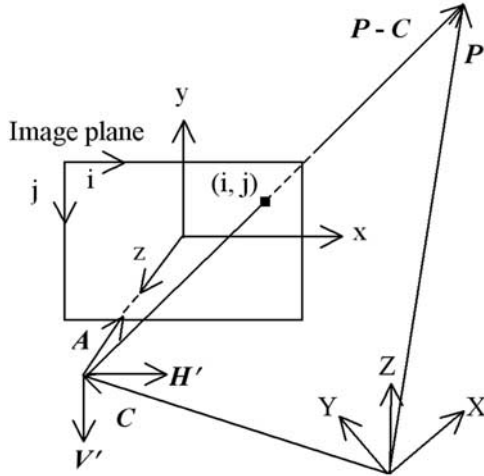


Figure 1. The CAHVOR model.

involved in the conversion. The conversion between the CAHVOR model and the DLT model is given in the appendix.

2. CAHVOR Camera Model and the Photogrammetric Model

2.1. CAHVOR Model

[6] Assume that the x and y axes are defined on the image plane in horizontal and vertical directions and the z axis is defined to form a right-handed image coordinate system (Figure 1). In a CAHVOR model, a unit vector H' and a unit vector V' are defined in the x direction and the negative y direction. The optical center of the image is at (h_c, v_c) in pixel expressed in column i and row j , which are approximately the half of the image dimension in horizontal and vertical directions. Note that in Figure 1 the image is positive and the row j column i system has its origin at the upper left corner.

[7] The first set of parameters in the CAHVOR model is the camera center vector C from the origin of the ground coordinate system (X - Y - Z) to the camera perspective center. The second set of parameters is the camera axis unit vector A , which is perpendicular to the image plane defined by H' and V' . Thus A , H' , and V' are mutually orthogonal.

[8] The third and fourth sets of parameters are two vectors H and V expressed as

$$H = h_s H' + h_c A, \quad (1a)$$

$$V = v_s H' + v_c A. \quad (1b)$$

These two vectors are also called horizontal and vertical information vectors. h_s and v_s equal to the focal length expressed in pixel [Yakimovsky and Cunningham, 1978]. Theoretically they should be identical for a detector with square pixels. However, because the calibration process does not enforce this condition and these two values are estimated and given in the calibration report, which are also called horizontal and vertical factors. Recommended by JPL, h_s is usually taken as f to compute depths from stereo images (M. Maimone, CAHVOR camera model informa-

tion, available at <http://robotics.jpl.nasa.gov/people/mwm/cahvor.html>).

[9] Using the orthogonality of A , H' and V' and equations (1a) and (1b), the parameters h_c , v_c , h_s and v_s can be calculated from vectors A , H and V with the following equations:

$$h_c = A \cdot H, \quad (1c)$$

$$v_c = A \cdot V, \quad (1d)$$

$$h_s = \|A \times H\|, \quad (1e)$$

$$v_s = \|A \times V\|, \quad (1f)$$

where “ \cdot ” denotes a scalar (dot) product of two vectors, “ \times ” denotes a cross product of two vectors, and “ $\|$ ” denotes the length of a vector.

[10] Letting P be the vector of the object point, the projection of the object point to its corresponding image point (i, j) using the CAHVOR model is represented as

$$i = \frac{(P - C) \cdot H}{(P - C) \cdot A}, \quad (2a)$$

$$j = \frac{(P - C) \cdot V}{(P - C) \cdot A}. \quad (2b)$$

The fifth set of parameters is the optical axis unit vector O , which is only used for lens-distortion correction in order for the distortion to be radial. If the image plane is perpendicular to optical axis, O is actually A . Defining a separate vector O for optical axis that is different from camera axis A allows for the possibility that the image plane and the optical axis are not exactly perpendicular to each other [Gennery, 1992]. O and A are calibrated independently in the JPL calibration process. However, their actual values are close.

[11] The sixth set of parameters R of the CAHVOR model contains radial lens distortion coefficients defined in the ground (object) coordinate system [Gennery, 1992]. Figure 2 is a 2-D profile that is on the plane formed by vectors $P - C$ and O . This plane cuts the image plane in a

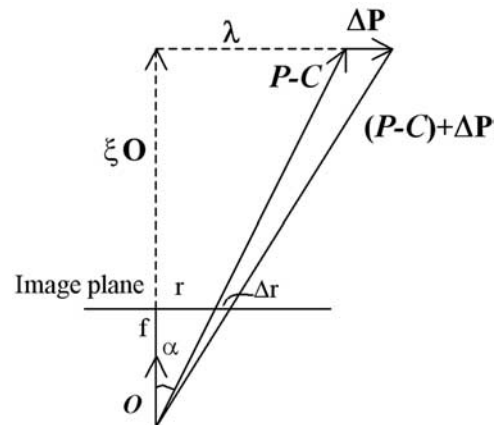


Figure 2. Radial lens distortion in the CAHVOR model.

radial direction. Equations (3) to (7) [Gennery, 1992] show how lens distortion coefficients are applied to correct the ground coordinates.

[12] The component of the vector $(\mathbf{P} - \mathbf{C})$ parallel to the optical axis is

$$\xi = (\mathbf{P} - \mathbf{C}) \cdot \mathbf{O}. \quad (3)$$

The vector perpendicular to the optical axis and pointing to the object point is

$$\lambda = (\mathbf{P} - \mathbf{C}) - \xi \mathbf{O}. \quad (4)$$

A parameter τ that changes monotonically with the angle α between the ray to \mathbf{P} and the optical axis is defined as

$$\tau = \tan^2 \alpha = \frac{\lambda \cdot \lambda}{\xi^2}. \quad (5)$$

Then, a proportionality coefficient μ is defined using a polynomial

$$\mu = \rho_0 + \rho_1 \tau + \rho_2 \tau^2. \quad (6)$$

The radial lens distortion produces a shift $\Delta \mathbf{P} = \mu \lambda$ that can be calculated using the last CAHVOR model parameter R (ρ_0, ρ_1, ρ_2) and the approximate point location. A decentering lens distortion is not included in this camera model. Finally, the point position in the ground coordinate system is corrected as [Gennery, 1992]

$$\mathbf{P}' = \mathbf{P} + \Delta \mathbf{P} = \mathbf{P} + \mu \lambda. \quad (7)$$

The corrected point \mathbf{P}' is then used in equations (2a) and (2b) instead of \mathbf{P} .

[13] As discussed above, each letter of the word CAHVOR represents either a vector or a set of three lens distortion coefficients of the camera model. Thus there are totally 18 component parameters in the CAHVOR model. Since \mathbf{A} and \mathbf{O} are unit vectors, there is one redundant parameter in each of them. The calibrated values of $h_c, h_s, v_c,$ and v_s are calculated from equations (1c) through (1f) and are usually provided in a calibration report.

[14] In order to model fisheye lenses, which have a very large field of view ($>100^\circ$), the CAHVOR model has been extended to CAHVORE model in which three more parameters are added for lens-distortion correction. The difference between CAHVOR and CAHVORE is that CAHVORE assumes the entering ray is projected at $r = f \sum_i e_i \alpha^i$ instead of $r = f \tan \alpha$, where α is the angle between the entering ray and the optical axis and r is the radial distance (see Figure 2), and i runs from 1 to 3 [Trebi-Ollennu et al., 2001]. For example, Hazcam (Hazard-avoidance Camera) cameras in the MER mission use the CAHVORE model.

[15] The CAHV, CAHVOR, and CAHVORE models are given for a particular pose of a camera with respect to a particular coordinate frame. When the camera is moved or the coordinate frame is changed, \mathbf{C} is translated and rotated, $\mathbf{A}, \mathbf{H}, \mathbf{V}, \mathbf{O}$ are rotated only, and R and E are unchanged.

2.2. Photogrammetric Model

[16] A photogrammetric model defines a set of interior orientation (IO) parameters and a set of exterior orientation (EO) parameters [Wolf, 1983; Mikhail et al., 2001]. The IO parameters include the focal length of the camera f and the

image coordinates of the principal point (x_o, y_o) where the optical axis intersects the image plane. The EO parameters are coordinates of the exposure center (X_C, Y_C, Z_C) in the ground-coordinate system and three rotation angles (ω, ϕ, κ) that describe the rotations about the three principal axes needed to rotate from the ground coordinate system X - Y - Z to the image coordinate system x - y - z (Figure 1).

[17] The transformation from the ground coordinates (X, Y, Z) to its image coordinates (x, y) is expressed by the following collinearity equations:

$$x - x_o = -f \frac{m_{11}(X - X_C) + m_{12}(Y - Y_C) + m_{13}(Z - Z_C)}{m_{31}(X - X_C) + m_{32}(Y - Y_C) + m_{33}(Z - Z_C)}, \quad (8a)$$

$$y - y_o = -f \frac{m_{21}(X - X_C) + m_{22}(Y - Y_C) + m_{23}(Z - Z_C)}{m_{31}(X - X_C) + m_{32}(Y - Y_C) + m_{33}(Z - Z_C)}, \quad (8b)$$

where m_{ij} are elements of a rotation matrix M and sine and cosine functions of the three angles:

$$M = \begin{bmatrix} \cos \phi \cos \kappa & \sin \omega \sin \phi \cos \kappa + \cos \omega \sin \kappa & -\cos \omega \sin \phi \cos \kappa + \sin \omega \sin \kappa \\ -\cos \phi \sin \kappa & -\sin \omega \sin \phi \sin \kappa + \cos \omega \cos \kappa & \cos \omega \sin \phi \sin \kappa + \sin \omega \cos \kappa \\ \sin \phi & -\sin \omega \cos \phi & \cos \omega \cos \phi \end{bmatrix}. \quad (8c)$$

The radial lens distortion is defined in the image plane as

$$\Delta r = k_0 r + k_1 r^3 + k_2 r^5, \quad (9)$$

where r is the radial distance of the image point from the principal point given by $r = \sqrt{(x - x_o)^2 + (y - y_o)^2}$, and k_i ($i = 0, 1, 2$) are the radial lens distortion coefficients that are provided in a camera calibration report. The corrections to image coordinates are

$$\Delta x = x \frac{\Delta r}{r}, \quad (10a)$$

$$\Delta y = y \frac{\Delta r}{r}. \quad (10b)$$

3. Conversion From the CAHVOR Model to the Photogrammetric Model

3.1. Computation of EO Parameters

[18] The position represented by the \mathbf{C} vector in the CAHVOR model is identical to the perspective center (X_C, Y_C, Z_C) in the photogrammetric model, which can be used directly.

[19] In order to calculate the rotation matrix in the photogrammetric camera model, we calculate the unit vectors \mathbf{H}' and \mathbf{V}' from equations (1a)–(1f):

$$\mathbf{H}' = \frac{\mathbf{H} - h_c \mathbf{A}}{h_s}, \quad (11a)$$

$$\mathbf{V}' = \frac{\mathbf{V} - v_c \mathbf{A}}{v_s} \quad (11b)$$

Then, the rotation matrix \mathbf{M} is calculated as

$$\mathbf{M} = \begin{bmatrix} \mathbf{H}' \\ -\mathbf{V}' \\ -\mathbf{A} \end{bmatrix} \quad (12)$$

on the basis of the property of the rotation matrix \mathbf{M} that the rows of matrix \mathbf{M} represent the basic unit vectors of the image coordinate system x - y - z in the ground coordinate system X - Y - Z (Figure 1) [Glassner, 1990; D. Gruber, The mathematics of the 3-D rotation matrix, available at <http://www.makegames.com/3drotation>]. Here, \mathbf{H}' , \mathbf{V}' and \mathbf{A} are row vectors. The three rotation angles (ω , ϕ , κ) are the Euler angle for rotations about the X , Y and Z axes in succession that make up the world to camera rotation matrix \mathbf{M} . They can be calculated from the rotation matrix using the formulas of Wolf [1983]. The angles (ω , ϕ , κ) are one of the commonly used definitions in the rotation matrix \mathbf{M} . Other angular definitions, including azimuth, tilt, and swing, are given by Wolf [1983].

[20] We can derive the collinearity equations from the CAHVOR projection equations to verify the above-calculated rotation matrix.

[21] Substituting \mathbf{H} in equation (2a), we have

$$\begin{aligned} i &= \frac{(\mathbf{P} - \mathbf{C}) \cdot (h_s \mathbf{H}' + h_c \mathbf{A})}{(\mathbf{P} - \mathbf{C}) \cdot \mathbf{A}} = \frac{h_s (\mathbf{P} - \mathbf{C}) \cdot \mathbf{H}' + h_c (\mathbf{P} - \mathbf{C}) \cdot \mathbf{A}}{(\mathbf{P} - \mathbf{C}) \cdot \mathbf{A}} \\ &= \frac{h_s (\mathbf{P} - \mathbf{C}) \cdot \mathbf{H}'}{(\mathbf{P} - \mathbf{C}) \cdot \mathbf{A}} + h_c \end{aligned}$$

or

$$i - h_c = h_s \frac{(\mathbf{P} - \mathbf{C}) \cdot \mathbf{H}'}{(\mathbf{P} - \mathbf{C}) \cdot \mathbf{A}} = -h_s \frac{(\mathbf{P} - \mathbf{C}) \cdot \mathbf{H}'}{(\mathbf{P} - \mathbf{C}) \cdot (-\mathbf{A})}.$$

If we multiply both sides of the above equation by the pixel size Δ_x (mm/pixel), it becomes

$$(i - h_c) \Delta_x = -(h_s \Delta_x) \frac{(\mathbf{P} - \mathbf{C}) \cdot \mathbf{H}'}{(\mathbf{P} - \mathbf{C}) \cdot (-\mathbf{A})},$$

which is

$$x = -f_x \frac{(\mathbf{P} - \mathbf{C}) \cdot \mathbf{H}'}{(\mathbf{P} - \mathbf{C}) \cdot (-\mathbf{A})}. \quad (13a)$$

From the projection equation (2b), in the same way we have

$$\begin{aligned} j &= \frac{(\mathbf{P} - \mathbf{C}) \cdot (v_s \mathbf{V}' + v_c \mathbf{A})}{(\mathbf{P} - \mathbf{C}) \cdot \mathbf{A}} = \frac{v_s (\mathbf{P} - \mathbf{C}) \cdot \mathbf{V}' + v_c (\mathbf{P} - \mathbf{C}) \cdot \mathbf{A}}{(\mathbf{P} - \mathbf{C}) \cdot \mathbf{A}} \\ &= \frac{v_s (\mathbf{P} - \mathbf{C}) \cdot \mathbf{V}'}{(\mathbf{P} - \mathbf{C}) \cdot \mathbf{A}} + v_c \end{aligned}$$

or

$$v_c - j = -v_s \frac{(\mathbf{P} - \mathbf{C}) \cdot \mathbf{V}'}{(\mathbf{P} - \mathbf{C}) \cdot \mathbf{A}} = -v_s \frac{(\mathbf{P} - \mathbf{C}) \cdot (-\mathbf{V}')}{(\mathbf{P} - \mathbf{C}) \cdot (-\mathbf{A})}.$$

Multiplying both sides of the above equation by the pixel size Δ_y (mm/pixel), it becomes

$$(v_c - j) \Delta_y = -(v_s \Delta_y) \frac{(\mathbf{P} - \mathbf{C}) \cdot (-\mathbf{V}')}{(\mathbf{P} - \mathbf{C}) \cdot (-\mathbf{A})}$$

or

$$y = -f_y \frac{(\mathbf{P} - \mathbf{C}) \cdot (-\mathbf{V}')}{(\mathbf{P} - \mathbf{C}) \cdot (-\mathbf{A})} \quad (13b)$$

Because \mathbf{H}' , $-\mathbf{V}'$ and $-\mathbf{A}$ are all unit vectors and perpendicular to each other, they can be put together to form a rotation matrix

$$\mathbf{M} = \begin{bmatrix} \mathbf{M}_1 \\ \mathbf{M}_2 \\ \mathbf{M}_3 \end{bmatrix},$$

where $\mathbf{M}_1 = \mathbf{H}'$, $\mathbf{M}_2 = -\mathbf{V}'$ and $\mathbf{M}_3 = -\mathbf{A}$. Then, equations (13a) and (13b) can be represented as

$$x = -f_x \frac{(\mathbf{P} - \mathbf{C}) \cdot \mathbf{M}_1}{(\mathbf{P} - \mathbf{C}) \cdot \mathbf{M}_3}, \quad (14a)$$

$$y = -f_y \frac{(\mathbf{P} - \mathbf{C}) \cdot \mathbf{M}_2}{(\mathbf{P} - \mathbf{C}) \cdot \mathbf{M}_3}, \quad (14b)$$

respectively. Here (x , y) are the image coordinates expressed in millimeters, whose origin is at the principal point of the image. The focal lengths f_x and f_y represent the horizontal and vertical focal lengths in millimeters. As is obvious, the CAHVOR-derived equations (14a) and (14b) are equivalent to the collinearity equations (8a) and (8b). Note that the image coordinates (x , y) in equations (13a), (13b), (14a), and (14b) are corrected for the principal point offset, corresponding to ($x - x_o$, $y - y_o$) in equations (8a) and (8b).

3.2. Computation of IO Parameters

[22] For the focal length f we can use either of the individual values $f_x (=h_s \Delta_x)$ or $f_y (=v_s \Delta_y)$ (from the above subsection) or their average. Also, we can use f_x and f_y for the calculation of x and y coordinates, respectively, in equations (8a) and (8b).

[23] In the derivation of equations (13a) and (13b), we calculated images coordinates (x , y) from pixel coordinates (i , j) using

$$x = (i - h_c) \Delta_x \quad (15a)$$

$$y = (v_c - j) \Delta_y. \quad (15b)$$

Generally, the calibrated h_c and v_c are not equivalent to the half of the image width and height (in pixels). The differences represent the principal point offsets. In photo-

grammetric processing, the image coordinates are calculated as

$$x = \left(i - \frac{\text{image_width}}{2} \right) \Delta_x - x_o, \quad (16a)$$

$$y = \left(\frac{\text{image_height}}{2} - j \right) \Delta_y - y_o. \quad (16b)$$

Given h_c and v_c , we can calculate the principal point coordinates as

$$x_o = \left(h_c - \frac{\text{image_width}}{2} \right) \Delta_x, \quad (17a)$$

$$y_o = \left(\frac{\text{image_height}}{2} - v_c \right) \Delta_y. \quad (17b)$$

When implementing equations (16a) to (17b), we should add 1 to both image_width and image_height if the up-left corner pixel is indexed as (0, 0).

3.3. Computation of Radial Lens Distortion Parameters

[24] From Figure 2, we can find

$$\frac{\Delta r}{\|\Delta P\|} = \frac{f}{|\xi|} = \frac{r}{\|\lambda\|}, \quad (18)$$

where $||$ is the absolute value of a scalar. From the figure, we also have

$$\Delta r = \|\Delta P\| \frac{r}{\|\lambda\|} = \mu \|\lambda\| \frac{r}{\|\lambda\|} = \mu r. \quad (19)$$

Substituting μ in the above equation by equation (6) and considering $\tau = \tan^2 \alpha = (r/f)^2$, we have

$$\Delta r = \left[\rho_0 + \rho_1 \left(\frac{r}{f} \right)^2 + \rho_2 \left(\frac{r}{f} \right)^4 \right] r = \rho_0 r + \frac{\rho_1}{f^2} r^3 + \frac{\rho_2}{f^4} r^5. \quad (20)$$

Comparing this equation with the lens distortion equation (9) of the photogrammetric model, we can derive the following relationship, by which we can calculate the radial lens distortion coefficients of the photogrammetric model from those of the CAHVOR model:

$$k_0 = \rho_0 \quad k_1 = \frac{\rho_1}{f^2} \quad k_2 = \frac{\rho_2}{f^4}. \quad (21)$$

[25] The CAHVOR model has more parameters (18 with two redundant parameters in unit vectors \mathbf{A} and \mathbf{O}) than the photogrammetric model (12). To give an in-depth comparison, we first compare the CAHV model and the photogrammetric model without considering lens distortion. The photogrammetric model has 9 independent parameters: 3 IO parameters and 6 EO parameters. On the other hand, the CAHV model has 12 parameters. Since \mathbf{A} is a unit vector, one parameter can be dropped. In the appendix, two

singularity constraints can be derived as equations (A4a) and (A4b). With these constraints, the number of independent parameters of the CAHV model is reduced to 9. However, the two singularity constraints were not applied in the JPL calibration process [Gennery, 1992]. In this case, the CAHV model allows horizontal and vertical focal lengths to be slightly different and vectors \mathbf{H}' and \mathbf{V}' are not perfectly orthogonal. Modeling lens distortion in the CAHVOR model using vector \mathbf{O} (not \mathbf{A}) allows the image plane to be not perfectly perpendicular to the optical axis, which adds two more independent parameters. Because of the above differences, the conversion from the CAHVOR model to the photogrammetric model may not be exact. However, we expect that the converted photogrammetric model should be able to produce a result at the same quality as the CAHVOR model or without significant differences. This is demonstrated in an example.

[26] The standard photogrammetric model is not suitable for modeling fisheye lens cameras. Therefore it may not be possible to convert the CAHVORE model to the photogrammetric model. However, during the MER mission, the stereo Hazcam images with the CAHVORE model will be warped to facilitate stereo matching. Lens-distortion correction is included in the warping process. The camera model of the warped images, also called linearized images, is reduced from CAHVORE to CAHV. We can convert the CAHV model of the warped images to the photogrammetric model and then perform photogrammetric mapping. The original Pancam (Panoramic Camera) and Navcam (navigation Camera) images are provided with CAHVOR models. We can use the conversion equations directly for these images. The warped versions of the Pancam and Navcam images will also be provided along with CAHV models. The conversion equations are applicable to these warped images as well.

4. Conversion From the Photogrammetric Model to the CAHVOR Model

[27] Inversely, given IO and EO parameters, we can convert the photogrammetric model to the CAHVOR model. The first vector \mathbf{C} is directly represented by the perspective center (X_C, Y_C, Z_C) in the photogrammetric model.

[28] Suppose that $\mathbf{M}_1, \mathbf{M}_2$ and \mathbf{M}_3 are the row vectors of the rotation matrix \mathbf{M} of the photogrammetric model. From equation (12) the following can be directly derived:

$$\mathbf{H}' = \mathbf{M}_1, \quad (22a)$$

$$\mathbf{V}' = -\mathbf{M}_2, \quad (22b)$$

$$\mathbf{A} = -\mathbf{M}_3. \quad (22c)$$

Using focal length f , we have

$$h_s = f/\Delta_x, \quad (23a)$$

$$v_s = f/\Delta_y. \quad (23b)$$

Table 1. Corresponding Parameters in the Photogrammetric Model and the CAHVOR Model

	Photogrammetric Model	CAHVOR Model
<i>Interior Orientation Parameters</i>		
Focal length	f	Embedded in \mathbf{H} and \mathbf{V} (h_s, v_s)
Principal point	(x_o, y_o)	Embedded in \mathbf{H} and \mathbf{V} (h_c, v_c)
<i>Lens Distortion Parameters</i>		
Center of distortion	Principal point (x_o, y_o)	Defined by R
Radial lens distortion coefficients	k_0, k_1, k_2	R (ρ_0, ρ_1, ρ_2)
<i>Exterior Orientation Parameters</i>		
Camera position	(X_C, Y_C, Z_C)	\mathbf{C}
Camera orientation	Three rotation angles ω, ϕ , and κ	\mathbf{A} , and embedded in \mathbf{H} and \mathbf{V} (\mathbf{H}' and \mathbf{V}')

In addition, h_c and v_c , can be calculated as

$$h_c = \frac{\text{image_width}}{2} + \frac{x_o}{\Delta_x}, \quad (24a)$$

$$v_c = \frac{\text{image_height}}{2} - \frac{y_o}{\Delta_y}. \quad (24b)$$

Finally, vectors \mathbf{H} and \mathbf{V} are calculated using equations (1a)–(1f).

[29] In the photogrammetric model there is only one optical axis define. Considering that \mathbf{O} and \mathbf{A} are very close in practice, we assume that \mathbf{O} is equal to \mathbf{A} in the converted CAHVOR model. The coefficients of lens distortion “vector” R (ρ_0, ρ_1, ρ_2) are calculated from the parameters (k_0, k_1, k_2) as

$$\rho_0 = k_0, \quad \rho_1 = k_1 f^2, \quad \rho_2 = k_2 f^4. \quad (25)$$

Table 1 summarizes the corresponding parameters in both models.

5. A Numerical Example

[30] We provide a numerical example of the camera model conversions in order to verify the method derived in this paper. A stereo pair of Kodak DCS 410 cameras were calibrated at JPL using the CAHVOR model. The calibrated camera system was used to collect simulated Mars rover images of a 1 km traverse for a rover localization study [Li et al., 2002]. A conversion from the CAHVOR model to the

photogrammetric model is performed for a bundle adjustment of the images based on the photogrammetric model.

[31] The image size is 762 columns by 506 rows and the pixel size is 0.01838 mm in both column and row directions. The nominal focal length is 28 mm. The calibration was carried out using a calibration frame with regularly distributed dots (control points) where 3-D positions are precisely surveyed. The camera-to-target distance is about 5 m. For the images used in this example, 258 control points for the left image and 271 control points for the right image were used in the calibration. The parameters of the CAHVOR model are given in Table 2. In this table, we also list the fractional difference in focal lengths $(h_s - v_s)/(0.5(h_s + v_s))$, the angle between \mathbf{H}' and \mathbf{V}' , and the angle between \mathbf{O} and \mathbf{A} . They should be 0, 90° and 0° for an ideal photogrammetric camera model. These values in Table 2 give an example that shows differences between the CAHVOR model and the photogrammetric model.

[32] We converted the CAHVOR model of the two cameras to a photogrammetric model using the equations derived above. The parameters of the photogrammetric model of the two cameras are shown in Table 3. The focal lengths f of the left and right cameras are the average values of the horizontal and vertical components f_x and f_y .

[33] In order to check the computational correctness of the conversion, we converted the photogrammetric model back to the CAHVOR model which is then compared to the original CAHVOR model. The converted \mathbf{C} and the original \mathbf{C} has no difference because the position of the optical center in the photogrammetric model is directly taken from the original \mathbf{C} in the conversion. The converted R and the original R have virtually no difference ($<10^{-16}$) because the conversions are direct computation without approximation

Table 2. Parameters of the CAHVOR Model of Two Kodak DCS 410 Cameras

	Left Camera	Right Camera
\mathbf{C} , m	3.451904, 3.258335, 1.254338	3.279361, 3.433116, 1.250847
\mathbf{A}	−0.698217, −0.681994, −0.217661	−0.703505, −0.677950, −0.213223
\mathbf{H}	−1378.872803, 894.719666, −106.732689	−1379.598022, 891.776123, −105.060280
\mathbf{V}	86.414558, 49.038635, −1620.883789	84.518219, 49.860332, −1615.635986
\mathbf{O}	−0.695858, −0.679843, −0.231508	−0.700455, −0.676578, −0.227166
R	0.000200, −0.108075, 0.086320	0.000196, −0.119485, 0.270073
h_s , pixel	1603.741455	1599.611816
h_c , pixel	375.790863	388.375336
v_s , pixel	1603.135498	1598.997559
v_c , pixel	259.023773	251.229248
Fractional difference in focal lengths	0.0094%	0.0096%
Angle between \mathbf{H}' and \mathbf{V}'	89.9914 degree	89.9993 degree
Angle between \mathbf{O} and \mathbf{A}	0.8142 degree	0.8215 degree

Table 3. Converted Parameters of the Photogrammetric Model

	Interior Orientation Parameters			Exterior Orientation Parameters	
	Left	Right		Left	Right
f , mm	29.4711992	29.39522016	X_C , m	3.451904	3.279361
x_O , mm	-0.09574394	0.13555868	Y_C , m	3.258335	3.433116
y_O , mm	-0.11071695	0.03254642	Z_C , m	1.254338	1.250847
k_0	0.0002	0.0002	ω , degree	-72.2993175	-72.5410442
k_1 , mm ⁻²	-0.00012443	-0.00012508	ϕ , degree	44.2841281	44.7088915
k_2 , mm ⁻⁴	0.00000011	0.00000012	κ , degree	166.5327547	166.7086386

introduced (equations (21) and (25)). The differences of A , H , V and O are $[0, -5.948 \times 10^{-7}, -1.898 \times 10^{-7}]^T$, $[0.172782, -0.249941, 0.225010]^T$ in pixel, $[0.059646, 0.032567, -0.295563]^T$ in pixel, $[-0.002359, -0.002152, 0.013847]^T$, respectively, for the left image; and $[0, -3.119 \times 10^{-7}, -9.810 \times 10^{-8}]^T$, $[0.209449, -0.224085, 0.022128]^T$ in pixel, $[0.050885, 0.041361, -0.300122]^T$ in pixel, $[-0.003050, -0.001372, 0.013943]^T$, respectively, for the right image. We can see that the differences of H and V are within one third of a pixel. A useful analysis is to observe the angular changes between the converted and original A , H , V and O , which the above differences can make. The angle between the converted and original A is 0.09 second for the left image and 0.05 second for the right image; that for H is 29.62 seconds s for the left image and 9.34 seconds s for the right image; that for V is 6.32 seconds s for the left image and 6.06 seconds s for the right image; and that for O is 0.8142 degree for the left image and 0.8215 degree for the right image. Overall, the differences caused by the model conversion are not significant. As demonstrated in the later sections, the converted model can support 3-D coordinate reconstruction at an accuracy level of a few millimeters in a calibration environment.

[34] In order to validate the conversion equations, we can check if for the same ground point, the given CAHVOR model and the converted photogrammetric model compute the same image coordinates in the stereo images. We back-projected the ground coordinates of control points of the calibration frame (258 control points for the left image and 271 control points for the right image) onto the images using the CAHVOR model equation (equations (2a) and (2b)) and the collinearity equation (equations (8a)–(8c)). We compared the back-projected image coordinates as well as the known image coordinates that were precisely measured and used in the calibration. The mean and maximum absolute

image coordinate differences are listed in Table 4. The result of CAHVOR versus known coordinates provides the accuracy information of camera calibration, while the other two (“Photogrammetry versus CAHVOR model” and “Photogrammetry versus known coordinates”) are for conversion assessment. The differences for the model comparison are all very small (less than 0.1 pixel), which is about the accuracy of the camera calibration as shown in the last two rows in Table 4 (“CAHVOR versus known coordinates”). Furthermore, they are rather random and do not supply meaningful information for analyzing error patterns and causes. As discussed in the previous section, the conversion is not a one to one conversion. However, from a practical application point of view, this 3-D to 2-D projection verifies that the converted photogrammetry model is as sufficiently accurate as the original CAHVOR model.

[35] Conversely, we can also check if for the same corresponding image points, the computed ground coordinates by the converted photogrammetric model are sufficiently close to the known coordinates of the points. We selected 257 control points and used their measured image coordinates to calculate the ground coordinates using the converted photogrammetric model and then compared them with their known 3-D coordinates. The mean absolute differences are 0.0023 m, 0.0022 m, and 0.0007 m in X, Y and Z, respectively, with corresponding maximum absolute differences of 0.0097 m, 0.0090 m, and 0.0042 m. Such a conversion accuracy is sufficient for many precision mapping applications.

6. Summary

[36] In this paper, we studied the relationship between the CAHVOR model and the photogrammetric model. We presented a conversion method between the two models.

Table 4. Comparison of Image Coordinates Calculated From the CAHVOR Model and the Converted Photogrammetric Model

Image Coordinate Comparison	Image Column and Row	Mean Abs. Coord. Difference, pixel	Max. Abs. Coord. Difference, pixel
Photogrammetric model versus CAHVOR model (left image)	i	0.0224	0.1071
	j	0.0587	0.1971
Photogrammetric model versus CAHVOR model (right image)	i	0.0285	0.1227
	j	0.0658	0.2080
Photogrammetric model versus known coordinates (left image)	i	0.0616	0.3113
	j	0.0852	0.2584
Photogrammetric model versus known coordinates (right image)	i	0.0682	0.2471
	j	0.0866	0.3261
CAHVOR model versus known coordinates (left image)	i	0.0530	0.2907
	j	0.0603	0.2218
CAHVOR model versus known coordinates (right image)	i	0.0571	0.2311
	j	0.0554	0.2263

A numerical example is given to validate the developed conversion equations. The conversion equations have been used at the Ohio State University Mapping and GIS Laboratory in bundle adjustment computations for Mars rover localization and landing site mapping. Such conversions are also inevitable when software systems using multiple sensor models are applied for planetary explorations.

Appendix A: Conversion Between the CAHVOR Model and the DLT Model

[37] Another photogrammetric model, the DLT (Direct Linear Transform) model, projects a ground point (X, Y, Z) to its image column and row coordinates (i, j) by [Karara, 1989]

$$i = \frac{L_1X + L_2Y + L_3Z + L_4}{L_9X + L_{10}Y + L_{11}Z + 1}, \quad (A1a)$$

$$j = \frac{L_5X + L_6Y + L_7Z + L_8}{L_9X + L_{10}Y + L_{11}Z + 1}. \quad (A1b)$$

[38] The DLT coefficients L_i ($i = 1, 2, 3 \dots 11$) in equations (A1a) and (A1b) can be computed directly from the collinearity equation (equations (8a)–(8c)). Inversely, the interior and exterior orientation parameters can be calculated from the DLT coefficients [Karara, 1989; Mikhail *et al.*, 2001]. The lens distortion in the DLT model is defined in the image domain.

[39] Without considering lens distortion, the photogrammetric model (equations (8a)–(8c)) has 9 independent parameters for an ideal frame camera. The DLT has 11 parameters. Using the relationship between the rows of the rotation matrix (orthogonal matrix), two singularity constraint equations were derived by Bopp and Krauss [1978] and reformulated by Mikhail *et al.* [2001] as

$$\begin{aligned} & (L_1^2 + L_2^2 + L_3^2) - (L_5^2 + L_6^2 + L_7^2) \\ & + \frac{(L_5L_9 + L_6L_{10} + L_7L_{11})^2 - (L_1L_9 + L_2L_{10} + L_3L_{11})^2}{L_9^2 + L_{10}^2 + L_{11}^2} = 0, \end{aligned} \quad (A2a)$$

$$\begin{aligned} & L_1L_5 + L_2L_6 + L_3L_7 \\ & - \frac{(L_1L_9 + L_2L_{10} + L_3L_{11})(L_5L_9 + L_6L_{10} + L_7L_{11})}{L_9^2 + L_{10}^2 + L_{11}^2} = 0. \end{aligned} \quad (A2b)$$

By enforcing the two constraint equations in a DLT calibration process, the dependencies of the extra 2 parameters are eliminated [Mikhail *et al.*, 2001], which results in an exact solution. However, in many practical applications, the two equations are not applied for simplicity of computation.

[40] In the CAHVOR model, let us use (X, Y, Z) to denote the position of vector \mathbf{P} , and (X_C, Y_C, Z_C) are that of \mathbf{C} . \mathbf{A} , \mathbf{H} , and \mathbf{V} , represented as (A_1, A_2, A_3) , (H_1, H_2, H_3) ,

and (V_1, V_2, V_3) , respectively. If lens distortions are not considered, the CAHVOR model can be converted to the DLT model by

$$\begin{aligned} L_1 &= LH_1, \\ L_2 &= LH_2, \\ L_3 &= LH_3, \\ L_4 &= -L(H_1X_C + H_2Y_C + H_3Z_C), \\ L_5 &= LV_1, \\ L_6 &= LV_2, \\ L_7 &= LV_3, \\ L_8 &= -L(V_1X_C + V_2Y_C + V_3Z_C), \\ L_9 &= LA_1, \\ L_{10} &= LA_2, \\ L_{11} &= LA_3, \end{aligned} \quad (A3)$$

where $L = -1/(A_1X_C + A_2Y_C + A_3Z_C)$.

[41] Conversely, the parameters in the CAHVOR model without lens distortions can be calculated from the DLT model using the following equations:

$$\begin{aligned} L^2 &= L_9^2 + L_{10}^2 + L_{11}^2, \\ \mathbf{C} &= \begin{bmatrix} X_C \\ Y_C \\ Z_C \end{bmatrix} = - \begin{bmatrix} L_1 & L_2 & L_3 \\ L_5 & L_6 & L_7 \\ L_9 & L_{10} & L_{11} \end{bmatrix}^{-1} \begin{bmatrix} L_4 \\ L_8 \\ 1 \end{bmatrix}, \\ \mathbf{A} &= \begin{bmatrix} L_9/L \\ L_{10}/L \\ L_{11}/L \end{bmatrix}, \\ \mathbf{H} &= \begin{bmatrix} L_1/L \\ L_2/L \\ L_3/L \\ L_5/L \\ L_6/L \\ L_7/L \end{bmatrix}, \\ \mathbf{V} &= \begin{bmatrix} L_1/L \\ L_2/L \\ L_3/L \\ L_5/L \\ L_6/L \\ L_7/L \end{bmatrix}. \end{aligned} \quad (A4)$$

The CAHV model, i.e., the CAHVOR model without lens distortions, has 12 parameters. One parameter can be dropped since \mathbf{A} is a unit vector. Similar to equations (A2a) and (A2b), two singularity constraint equations can be established as

$$\begin{aligned} & (H_1^2 + H_2^2 + H_3^2) - (V_1^2 + V_2^2 + V_3^2) + (V_1A_1 + V_2A_2 + V_3A_3)^2 \\ & - (H_1A_1 + H_2A_2 + H_3A_3)^2 = 0, \end{aligned} \quad (A5a)$$

$$(H_1V_1 + H_2V_2 + H_3V_3) - (H_1A_1 + H_2A_2 + H_3A_3) \cdot (V_1A_1 + V_2A_2 + V_3A_3) = 0. \quad (\text{A5b})$$

[42] If the above two equations are enforced in the CAHVOR model calibration, the dependences between the CAHV parameters can be eliminated. However, the constraint equations are not applied in the JPL calibration process. Thus the CAHVOR model handles variations from the ideal frame camera, which is discussed in the paper.

[43] **Acknowledgments.** The CAHVOR-calibration data of the two Kodak cameras used in this paper were provided by Clark Olson, who was formerly a researcher at JPL and is now with Washington University. The research was partially supported by a contract from JPL. Collaboration with Larry Matthies of JPL is appreciated. We appreciate constructive comments from the reviewers.

References

- Bopp, H., and H. Krauss (1978), An orientation and calibration method for non-topographic applications, *Photogramm. Eng. Remote Sens.*, **9**, 1191–1196.
- Gennery, D. B. (1992), Least-squares camera calibration including lens distortion and automatic editing of calibration points, paper presented at Workshop on Calibration and Orientation of Cameras in Computer Vision, XVII Congress of the International Society of Photogrammetry and Remote Sensing, Washington, D. C., 2 Aug.
- Glassner, A. S. (1990), *Graphics Gems*, Academic, San Diego, Calif.
- Karara, H. M. (1989), *Non-Topographic Photogrammetry*, Am. Soc. for Photogramm. and Remote Sens., Falls Church, Va.
- Kirk, R. L., et al. (1999), Digital photogrammetric analysis of the IMP camera images: Mapping the Mars Pathfinder landing site in three dimensions, *J. Geophys. Res.*, **104**, 8869–8887.
- Li, R., F. Ma, F. Xu, L. H. Matthies, C. F. Olson, and R. E. Arvidson (2002), Localization of Mars rovers using descent and surface-based image data, *J. Geophys. Res.*, **107**(E11), 8004, doi:10.1029/2000JE001443.
- Li, R., K. Di, L. H. Matthies, R. Arvidson, W. M. Folkner, and B. A. Archinal (2004), Rover localization and landing site mapping technology for the 2003 Mars Exploration Rover Mission, *Photogramm. Eng. Remote Sens.*, **70**(1), 77–90.
- Mikhail, E. M., J. S. Bethel, and J. D. McGlone (2001), *Introduction to Modern Photogrammetry*, John Wiley, New York.
- Trebi-Ollennu, A., T. Huntsberger, Y. Cheng, E. T. Baumgartner, B. Kennedy, and P. Schenker (2001), Design and analysis of a Sun sensor for planetary rover absolute heading detection, *IEEE Trans. Robotics Autom.*, **17**, 939–947.
- Wolf, P. R. (1983), *Elements of Photogrammetry*, McGraw-Hill, New York.
- Yakimovsky, Y., and R. Cunningham (1978), A system for extracting three-dimensional measurements from a stereo pair of TV cameras, *Comput. Graphics Image Process.*, **7**, 195–210.

K. Di and R. Li, Mapping and GIS Laboratory, Civil and Environmental Engineering and Geodetic Science, 470 Neil Avenue, Ohio State University, Columbus, OH 43210, USA. (di.2@osu.edu)